



1 **The Teddy-Tool v1.0: temporal disaggregation of daily climate** 2 **model data for climate impact analysis**

3 Florian Zabel¹, Benjamin Poschlod²

5 ¹Ludwig-Maximilians-Universität München (LMU), Department of Geography, Luisenstr. 37, 80333 Munich,
6 Germany

7 ²Research Unit Sustainability and Climate Risks, Center for Earth System Research and Sustainability, Universität
8 Hamburg, Grindelberg 5, 20144 Hamburg, Germany

9 Correspondence to: Florian Zabel (f.zabel@lmu.de)

10 **Abstract**

11 Climate models provide required input data for global or regional climate impact analysis in aggregated
12 form, often on a daily basis to save space on data servers. Today, many impact models work with daily
13 data, however, sub-daily climate information is getting increasingly important for more and more
14 models from different sectors, such as the agricultural, the water, and the energy sector. Therefore,
15 the open source Teddy-Tool (**t**emporal **d**isaggregation of **d**aily climate model data) has been developed
16 to disaggregate (temporally downscale) daily climate data to sub-daily hourly values for temperature,
17 precipitation, humidity, longwave radiation, shortwave radiation, surface pressure and wind speed.
18 Thereby, mass and energy are strictly preserved by the Teddy-Tool to exactly reproduce the daily
19 values from the climate models. Here, we describe and document the temporal disaggregation, which
20 is based on globally available bias-corrected hourly reanalysis WFDE5 data from 1980-2019 to take
21 specific local and seasonal features of the diurnal course empirically into account. The physical
22 dependency between variables is preserved, since the diurnal profile of all variables is taken from the
23 same, most similar meteorological day of the historical reanalysis dataset. We perform a sensitivity
24 analysis of different time window sizes used for finding the most similar meteorological day in the past.
25 In addition, we perform a cross-validation, autocorrelation and extreme value analysis for 30 globally
26 distributed samples around the world, representing different climate zones. The validation shows that
27 Teddy is able to reproduce historical diurnal courses with high correlations >0.9 for all variables, except
28 for wind speed (>0.75) and precipitation (>0.5). Consequently, sub-daily data provided by the Teddy-
29 Tool could make climate impact assessments more robust and reliable.

30 **Introduction**

31 Sub-daily climate data is becoming increasingly important in climate impact analysis. This type of data,
32 which captures variations in temperature, precipitation, and other weather variables at intervals of
33 less than a day, can provide a more detailed representation of local and regional climate conditions
34 and temporal variations. This information can be crucial for evaluating the impacts of climate change
35 on various sectors, such as agriculture, water resources, energy production, and human health (Golub
36 et al., 2022; Trinanes and Martinez-Urtaza, 2021; Colón-González et al., 2021; Tittensor et al., 2021;
37 Byers et al., 2018; Jägermeyr et al., 2021; Poschlod and Ludwig, 2021; Degife et al., 2021). A better
38 representation of the diurnal course of temperature, extreme precipitation events, and other weather
39 variables are also important for adaptation assessments which depend on behavior or processes with
40 high temporal dynamics, such as the energy demand, labor activity, the heat stress of crops or flood
41 events (Minoli et al., 2022; Zabel et al., 2021; Reed et al., 2022; Orlov et al., 2021; Franke et al., 2022).



42 Research has shown that using sub-daily climate data can result in more robust and reliable impact
43 assessments compared to using daily data (Orlov et al. 2023).

44 Today, most climate model data are available for download at daily resolution because of the high
45 storage requirements for sub-daily climate data. However, the demand for sub-daily data is increasing
46 due to lower costs for storage and computing resources. Different methods exist to disaggregate
47 available daily climate data to sub-daily, most often hourly values. These can be roughly divided into
48 statistical methods, weather generators, and mechanistic approaches, although mixed forms also exist
49 (Förster et al., 2016).

50 Mechanistic methods use regional climate models to dynamically downscale atmospheric conditions
51 in time and space, usually for a limited area (Vormoor and Skaugen, 2013; Liu et al., 2011; Kunstmann
52 and Stadler, 2005). Weather generators generate synthetic sequences of hourly weather variables by
53 using random number generators that match statistics (Ailliot et al., 2015; Mezghani and Hingray,
54 2009). Various statistical methods exist for temporal disaggregation of daily climate data, ranging from
55 simple interpolations or deterministic approaches to non-parametric approaches and methods that
56 derive statistical relationships from historical data (Breinl and Di Baldassarre, 2019; Debele et al., 2007;
57 Förster et al., 2016; Görner et al., 2021; Liston and Elder, 2006; Park and Chung, 2020; Verfaillie et al.,
58 2017; Poschlod et al., 2018; Zhao et al., 2021). Each of these methods has its own advantages and
59 limitations, and the choice of method depends on factors such as the specific needs of the impact
60 assessment, the quality of the available data, and computational resources.

61 Here, we introduce the Teddy-Tool (**t**emporal **d**isaggregation of **d**aily climate model data), which uses
62 statistical methods for temporal disaggregation of daily climate model data. Existing statistical
63 approaches are often only valid for a specific location and cannot be applied globally. In addition,
64 available disaggregation tools often focus on only one variable and therefore do not consider physical
65 interdependencies between different variables, such as precipitation, humidity, temperature, and
66 radiation. Teddy has been specifically developed as a globally applicable tool for climate impact
67 studies. For this purpose, Teddy strictly preserves mass and energy of daily climate model data for each
68 variable throughout the disaggregation procedure. Teddy additionally aims at taking regional and
69 seasonal climate characteristics into account and considers the physical consistency between
70 variables.

71 In principal, the Teddy-Tool can be used with any climate input, but has particularly been used so far
72 with bias corrected daily CMIP6 climate data (Eyring et al., 2016) for historical time periods and future
73 scenarios from the ISIMIP (Inter-Sectoral Impact Model Intercomparison Project), which provides bias
74 corrected and trend-preserved climate data (Lange, 2019) and offers a framework for consistently
75 projecting the impacts of climate change across affected sectors and spatial scales (Warszawski et al.,
76 2014). To guarantee cross-sectoral consistency, all sectors are provided with the same climate data.
77 Within ISIMIP, some models from different sectors have expressed their need for sub-daily climate
78 data, including the agricultural and the energy sector. Teddy represents an easy-to-use tool that can
79 be applied for climate impact assessments in different sectors that allows a physically consistent
80 temporal disaggregation of the daily ISIMIP climate model data. The Teddy-Tool has been written in
81 Matlab and is available open source via Zenodo (<https://doi.org/10.5281/zenodo.7679149>).

82

83



84 **1. Temporal disaggregation**

85 Teddy uses an empirical approach, which applies the region-specific diurnal course from the most
 86 similar day in the past to daily climate model data for a day of interest. Teddy has been developed
 87 specifically to disaggregate daily bias-corrected climate model data from the ISIMIP project at 0.5°
 88 spatial resolution for air temperature (tas), humidity (hurs), shortwave radiation (rsds), longwave
 89 radiation (rlds), air pressure (ps), windspeed (sfcwind), and precipitation (pr) (Lange, 2019). For air
 90 temperature, the daily maximum and minimum values (tasmax, tasmin) are additionally provided.
 91 ISIMIP provides data for different historical and future time periods and scenarios for the climate
 92 models GFDL-ESM4, IPSL-CM6A-LR, MPI-ESM1-2-HR, MRI-ESM2-0, and UKESM1-0-LL. As a reference,
 93 globally available hourly bias-corrected reanalysis WFDE5 data (1980-2019) are used at 0.5° spatial
 94 resolution to identify the most similar meteorological day in the past for a specific location (Cucchi et
 95 al., 2020). The diurnal profile of the most similar day is subsequently applied to the daily climate model
 96 data for each of the variables. In the following, the procedure is explained:

97 In a first precalculation step, in order to minimize computational resources, hourly WFDE5 data are
 98 aggregated to daily values and stored as NetCDF files. The daily aggregation uses mean values for all
 99 variables and daily sums for precipitation. In addition, rainfall and snowfall fluxes must be summed up
 100 for WFDE5. Daily maximum and minimum temperature are calculated from the hourly data. Units of
 101 climate inputs are converted to match the Teddy output (see Tab. 1). For the conversion of specific
 102 humidity to relative humidity, the Buck equation is applied (Buck, 1981).

103 Table 1: Variables and units of used hourly (h) and daily (d) climate data and the Teddy output. For
 104 WFDE5, the specific variable name is provided in brackets. WFDE5 variables have instantaneous values,
 105 while SWdown, LWdown, Rainf and Snowf have average values over the next hour at each time step.

Variable	WFDE5 (h)	ISIMIP Climate Model (d)	Teddy (flexible)
tas	K (Tair)	K	K
tasmin	-	K	-
tasmax	-	K	-
hurs/huss	kg/kg (Qair)	%	%
rsds	W m ⁻² (SWdown)	W m ⁻²	W m ⁻²
rlds	W m ⁻² (LWdown)	W m ⁻²	W m ⁻²
pr	kg m ⁻² s ⁻¹ (Rainf+Snowf)	kg m ⁻² s ⁻¹	mm timestep ⁻¹
ps	Pa (PSurf)	Pa	hPa
sfcwind	m s ⁻¹ (Wind)	m s ⁻¹	m s ⁻¹

106

107 After reading the daily climate model data for the selected location (latitude/longitude) that
 108 determines a specific grid cell at 0.5° resolution, the daily mean values of all ISIMIP variables (see Tab.
 109 1) are compared to the aggregated daily values of WFDE5 for a specific time step in order to identify

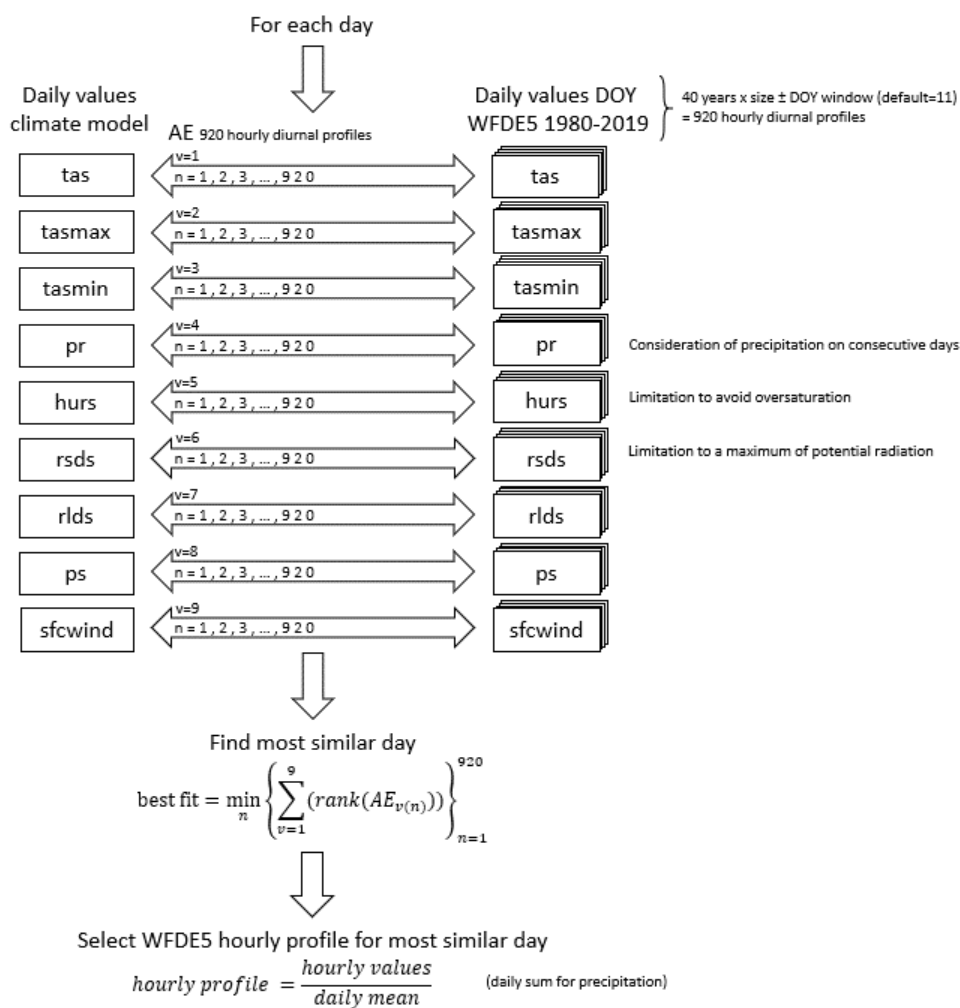


110 the most similar meteorological day. For the comparison, a day-of-year (DOY) window can be selected
111 by the user that allows for a selection of days around the DOY of the actual time step. By default, the
112 DOY window size is set to 11, which means a sequence of ± 11 days around the actual DOY. As a result,
113 23 days are selected from each of the 40 WFDE5 reference years (1980-2019). These 920 days now
114 serve as the basic population for further calculations (Fig. 1). In a next step, the climate model day of
115 interest and the basic population of 920 WFDE5 days are classified according to their precipitation
116 state. As climate models tend to produce too many days with low-intensity precipitation called “drizzle
117 bias” (Chen et al., 2021), days with aggregated daily precipitation values below 1 mm per day are
118 considered as dry days (Sun et al., 2006). Depending on the precipitation state of the previous day, the
119 day of interest and the following day, there are eight classes: dry-dry-dry, dry-dry-wet, wet-dry-dry,
120 wet-dry-wet, dry-wet-dry, dry-wet-wet, wet-wet-dry, and wet-wet-wet. This step is included to better
121 reproduce the inter-day connectivity of precipitation (Li et al., 2018). Only days with the same
122 precipitation class as the climate model day of interest are selected for the further course. Next, the
123 absolute error between daily climate model and aggregated daily WFDE5 data for each variable is
124 calculated for the remaining basic population and ranked in ascending order. The ranks over all
125 variables are cumulated for each day of the basic population. The most similar meteorological day is
126 determined as the day with the lowest cumulated ranks (Fig. 1). Finally, the hourly values are taken
127 from the most similar day of the WFDE5 reference dataset for each variable and divided by the WFDE5
128 daily mean value of the selected day, in order to refer to relative diurnal profiles without absolute
129 variations (Fig. 1). The hourly profile is then applied for each variable to the daily mean value from the
130 climate model. Thus, the daily mean is conserved.

131 For temperature, the resulting hourly temperature is further scaled between the provided minimum
132 and maximum. The scaling is performed in a way that the daily mean value is preserved with an
133 accuracy of four decimals. Relative humidity is limited to 100%, again under preserving the daily mean
134 value.

135 Large selected DOY windows increase the basic population, but on the other side might distort climatic
136 characteristics with a strong seasonal course such as shortwave radiation values for the actual DOY.
137 Therefore, we preprocessed hourly potential (cloud free) solar radiation for each DOY globally at 0.5°
138 spatial resolution. This data is used as upper bound to limit the resulting hourly values for the
139 corresponding DOY, while the daily mean value is preserved.

140 In a final step, hourly values can again be aggregated to the time step set by the user (possible: 1, 2, 3,
141 4, 6, 8, 12).



142

143 Figure 1: Procedure to identify the most similar meteorological day in the population of reference data
 144 for the default DOY window of ± 11 days around the actual DOY.

145 In rare cases, precipitation cannot be distributed, due to failing precipitation in the reference data. To
 146 handle this exception, several options are implemented. First, the DOY window is automatically
 147 expanded to ± 50 days around the actual DOY. If this doesn't help, a linear regression between the
 148 precipitation amount and the duration is performed for the specific location across the entire data
 149 spectrum. The linear regression determines the usual duration of the selected precipitation event.
 150 Subsequently, an hour is randomly selected for the start of the precipitation event. In order to reduce
 151 possible physical inconsistencies with other variables that could lead to implications in impact models,
 152 the precipitation is only distributed to hours at nighttime (without solar radiation).

153 Precipitation values below 1 mm day^{-1} are also disaggregated to sub-daily values in order to ensure
 154 mass and energy conservation. If no historical precipitation event is found for this case, precipitation

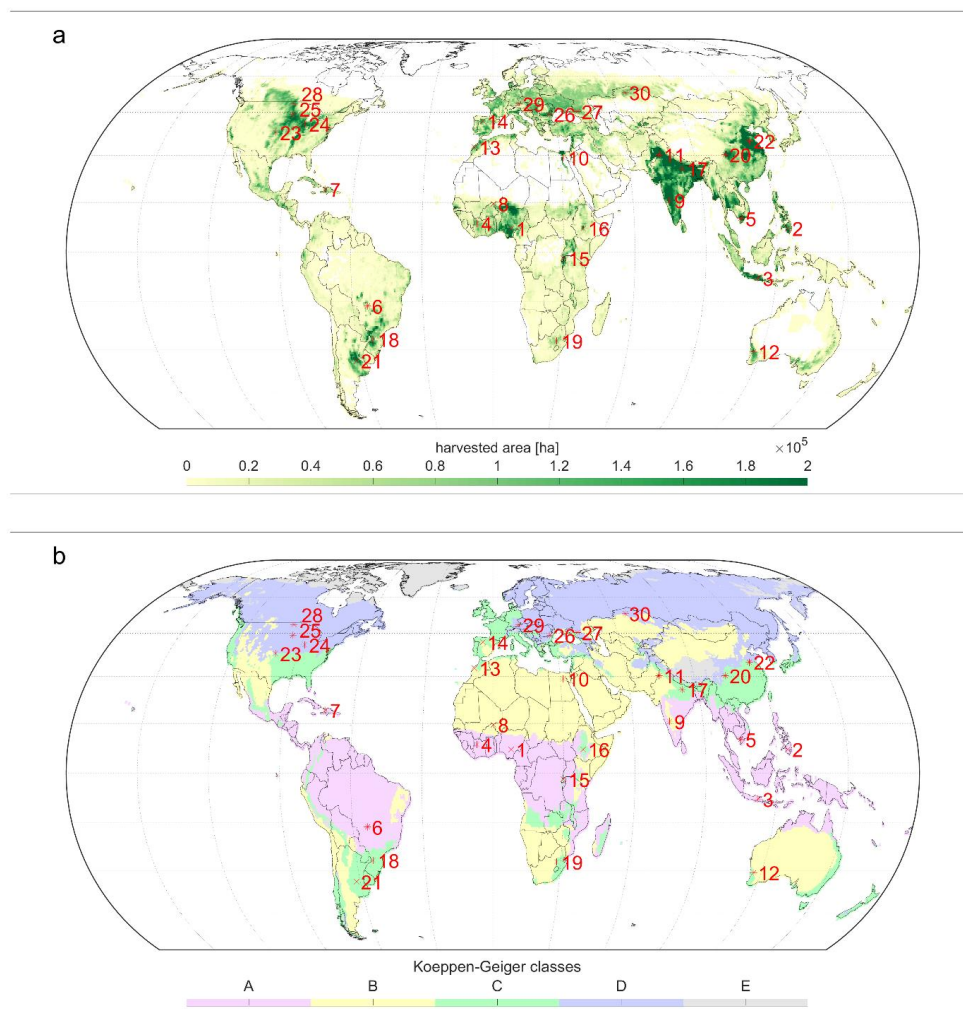


155 noise is randomly distributed to an hour at nighttime. If no hour without radiation occurs (e.g. high
156 latitudes in northern summer), the precipitation is distributed to local midnight.

157 The calculation procedure can be performed either for universal time (UT) or for local solar time (LST).
158 The latter divides the world into equal time zones of 15° with the central time zone (+7.5°) at
159 Greenwich.

160 **2. Validation**

161 In a first step, a cross-validation is carried out for 30 globally distributed samples (Fig. 2) for the year
162 2010. Therefore, WFDE5 data for 2010 aggregated to daily values serves as an input. The same year is
163 excluded from the basic population during the cross-validation. As a result, it can be tested how well
164 WFDE5 hourly values for the year 2010 are reproduced with the basic population of all other years.
165 The 30 samples are chosen to represent globally relevant agricultural production regions in different
166 climate zones (Fig. 2). To evaluate the sensitivity of the different DOY window sizes, we run the cross-
167 validation with different DOY window sizes, ranging from 1 to 25, in steps of two, including the option
168 to disable the DOY window (DOY window size = 0). In order to additionally validate the performance
169 for extreme events, we perform a second cross-validation for all available 40 years (1980-2019) with
170 DOY window sizes of 11 and 25 for sample location 29, located in Southern Germany.

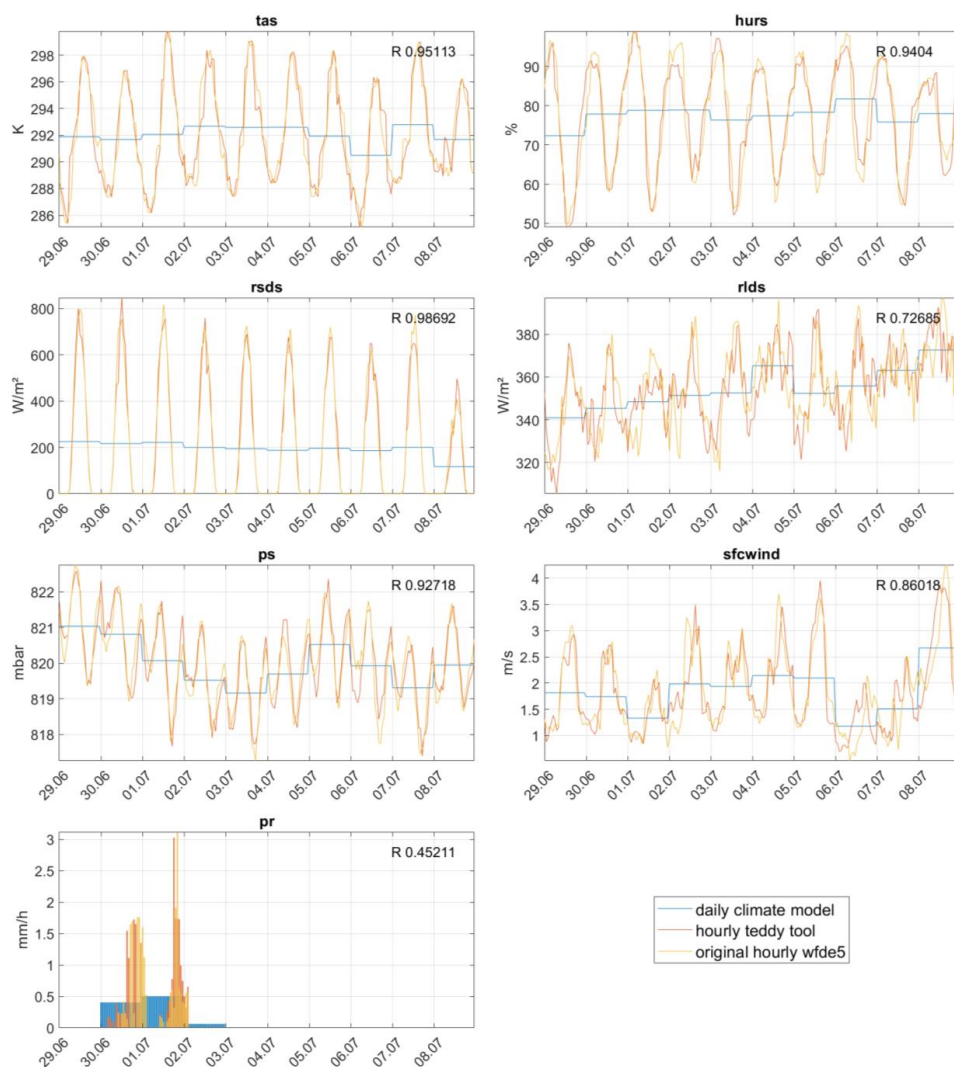


171

172

173 Figure 2: Distribution of 30 global samples used for the cross-validation on (a) annual total harvested
174 area of rainfed and irrigated crops in hectare per pixel at a 30 arc-minute grid (Portmann et al., 2010)
175 and (b) for Koeppen-Geiger climate zones calculated for 1980-2019 WFDE5 temperature and
176 precipitation values (Beck et al., 2018). Samples are ordered by climate zone affiliation and their
177 distance to the equator.

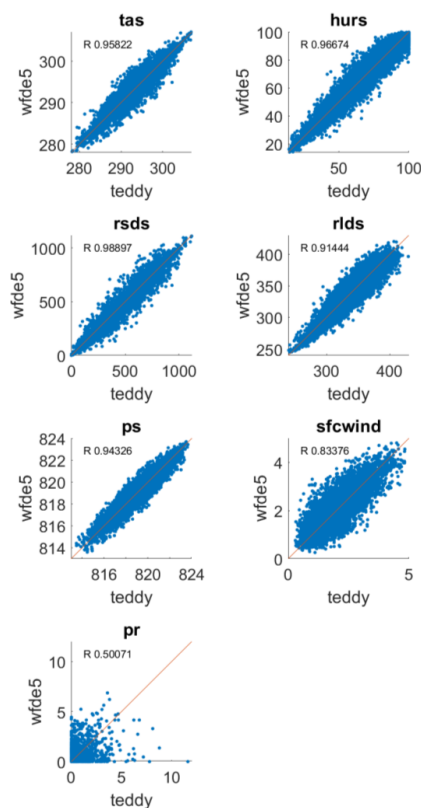
178 As an example for sample location 16 in Ethiopia, Fig. 3 shows the results of the temporal
179 disaggregation series for the cross-validation for a 10-day time series in 2010 in comparison with the
180 daily climate input and the original hourly WFDE5 data. The hourly courses show high correlations for
181 the randomly selected time series for all variables (Fig. 3 and scatterplots in Fig. 4 for the entire year).



182

183 Figure 3: Time-series for all variables comparing daily climate model data, disaggregated hourly results
184 of Teddy from the performed cross-validation and the original hourly WFDE5 data, shown for sample
185 location 16 in Ethiopia with a DOY window size of 7 for the 10-day period 29.06. – 08.07.2010. The
186 Pearson correlation coefficient (R) is displayed for the shown time period for each variable.

187

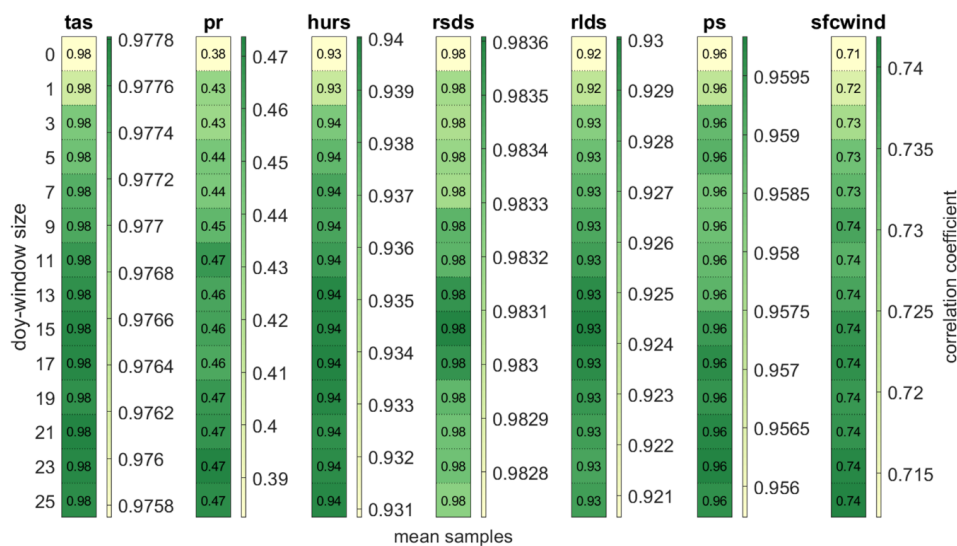


188

189 Figure 4: Hourly values for the year 2010 between disaggregated values generated by the Teddy-Tool
190 and the original WFDE5 data used for the cross-validation, exemplarily for sample 16 in Ethiopia with
191 a DOY window size of 7.

192 2.1 Sensitivity analysis DOY window size

193 The sensitivity analysis averaged over all 30 samples shows that the Pearson correlation coefficient of
194 hourly values for the year 2010 show high correlations for all variables ($r > 0.9$), except windspeed
195 ($r > 0.7$) and precipitation ($r > 0.4$), which are generally are the most difficult variables for disaggregation
196 (Fig 5). The selected DOY window size has an effect on the quality of the results. While no DOY window
197 (size=0) results in the lowest correlation coefficient across all variables, the DOY window size does not
198 significantly affect the correlation except for precipitation and wind speed (Fig. 5).



199

200 Figure 5: Pearson correlation coefficient for different DOY window sizes averaged over all 30 samples
 201 for the year 2010 for all variables being disaggregated to hourly values. The scaling of the colorbar
 202 differs between variables.

203 For precipitation, the impact of the DOY window size on the correlation varies between regions. Larger
 204 DOY windows are mainly beneficial for precipitation in tropical and arid regions, while in regions with
 205 pronounced seasons, the correlation might decrease with larger DOY window size (Fig. 6). The results
 206 also show that the correlation for precipitation is generally larger in tropical regions than in continental
 207 regions.

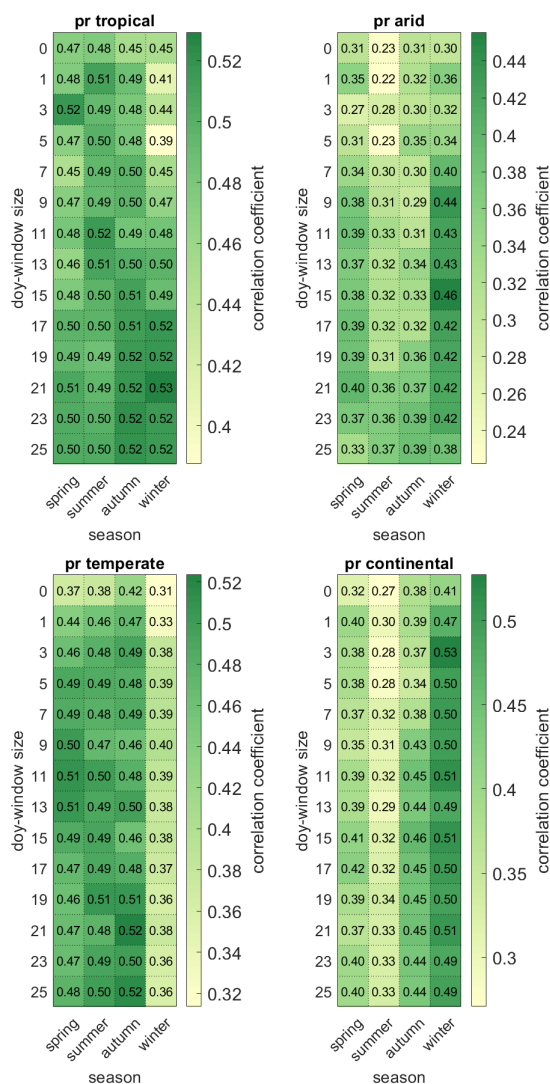


208

209 Figure 6: Pearson correlation coefficient for different DOY window sizes averaged over the samples for
 210 each Koeppen-Geiger climate zone (A=tropical, B=arid, C=temperate, D=continental).



211 While hourly precipitation can be best reproduced for winter seasons in continental and arid regions,
 212 winter seasons show the lowest correlation for temperate regions. Tropical regions only show
 213 relatively low variations over the year, independently from the selected DOY window size (Fig. 7).
 214 Especially in arid regions, the length of the DOY window size affects the results differently in different
 215 seasons. Here, larger DOY windows decrease the correlation during the rainy season (winter and
 216 spring), while correlation is increased during the dry season (summer and autumn).



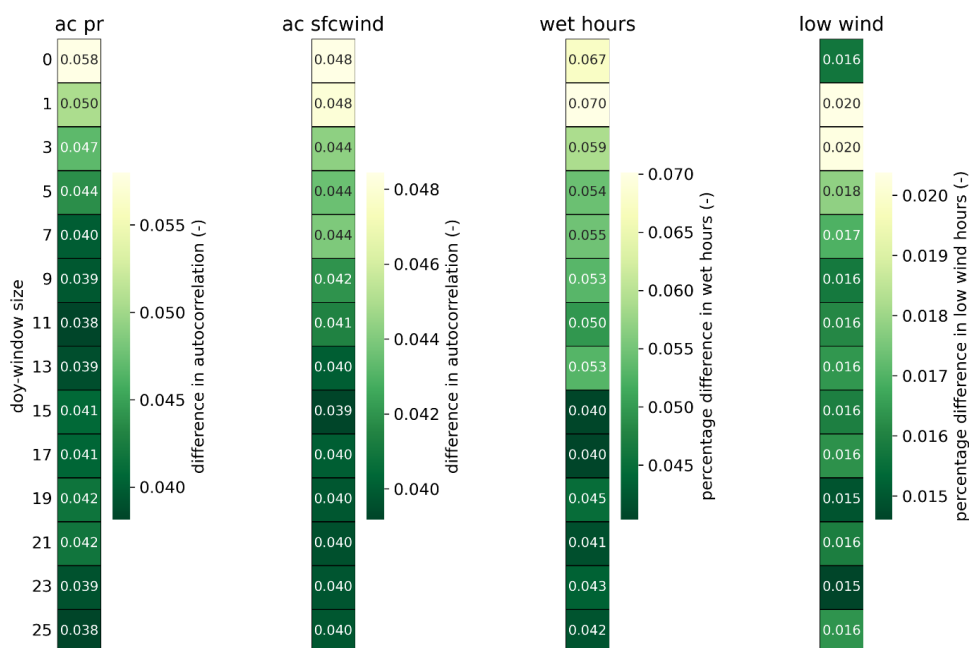
217

218 Figure 7: Pearson correlation coefficient for different DOY window sizes averaged over the samples for
 219 the four seasons (spring=MAM, summer=JJA, autumn=SON, winter=DJF). The shift of the seasons
 220 between Northern and Southern hemisphere is considered. The heatmap is averaged over the samples
 221 for each Koeppen-Geiger climate zone (A=tropical, B=arid, C=temperate, D=continental).



222 Furthermore, we evaluate the sensitivity of the DOY window size to the reproduction of temporal
 223 autocorrelation (Fig. 8). Therefore, the autocorrelation over lag times between one and 24 hours is
 224 calculated for precipitation and wind speed. Autocorrelation refers to the similarity of a time series to
 225 a lag duration shifted version of the same time series. This allows sub-daily patterns and inter-hour
 226 connectivity to be statistically captured and validated in time series of precipitation and wind speed.
 227 In addition, we also check the reproduction of wet hours (precipitation above 0.1 mm h^{-1}) in 2010 and
 228 the number of hours with low wind speeds (sfcwind $< 2.5 \text{ m s}^{-1}$) referring to the typical cut-in wind
 229 speed of wind turbines.

230 Here, we find that short DOY window sizes below 5 days are not beneficial to all statistics. The
 231 autocorrelation of precipitation (wind speed) is reproduced more accurately with window sizes of 9
 232 days or longer. The number of wet hours is better recreated with window sizes above 15 days. For
 233 hours with low wind speed, a minor improvement is found above 9 days.



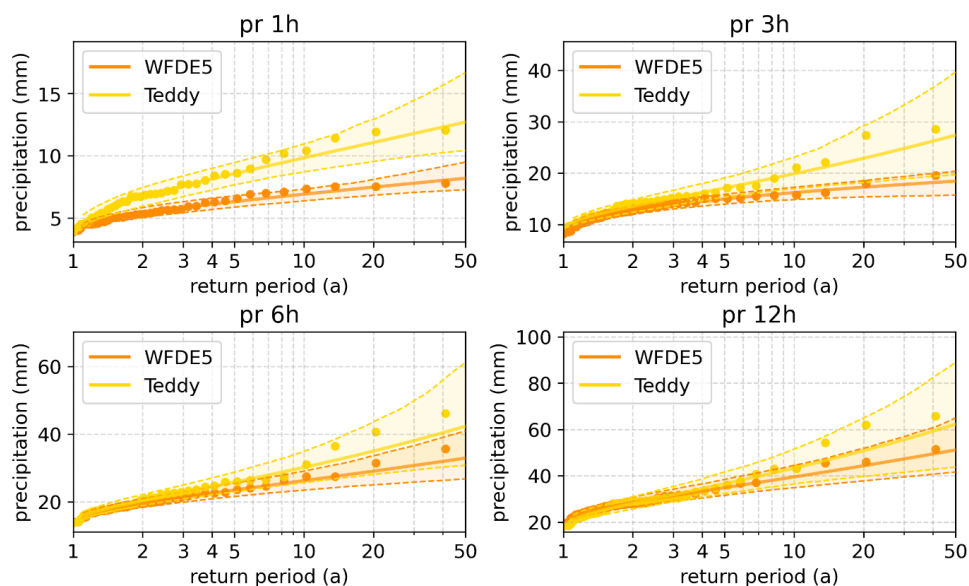
234

235 Figure 8: Extended validation statistics for the sensitivity analysis of the DOY window size for the year
 236 2010. The difference in autocorrelation refers to the average over all 30 stations and lag durations
 237 between one and 24 hours. Wet hours are defined as precipitation intensities above 0.1 mm h^{-1} and
 238 low wind speeds refer to hours with sfcwind $< 2.5 \text{ m s}^{-1}$.

239 As the ISIMIP data base is used for future impact modelling and historical attribution science (Mengel
 240 et al., 2021), extremes are of major interest for the community. The ability of global climate models to
 241 simulate sub-daily extremes is limited and depends on the variable of interest and the spatio-temporal
 242 conditions of the extreme and the respective model setup (Wehner et al., 2021; Kumar et al., 2015;
 243 Wang and Clow, 2020). However, in this validation, we need to evaluate how the Teddy-Tool is able to
 244 preserve the statistics of sub-daily extreme values. Therefore, we select precipitation as variable of
 245 interest. Figure 9 shows the reproduction of sub-daily precipitation extremes for 1980 – 2019 for

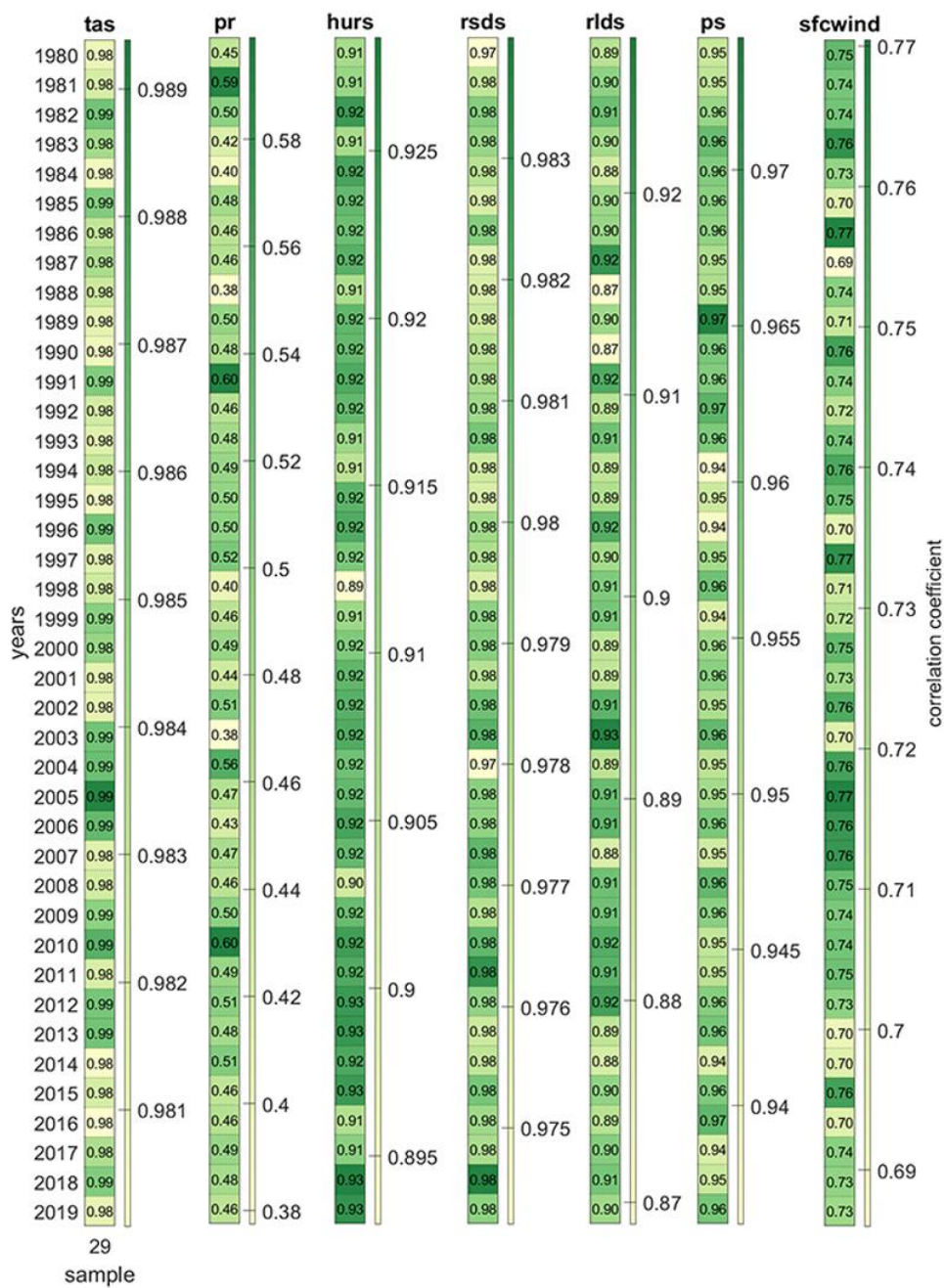


246 sample location 29 in southern Germany, where Teddy is run with a DOY window size of 11 days. The
247 40 annual maxima are extracted from the original and the disaggregated data. Additionally, the
248 Generalized Extreme Value (GEV) distribution is fitted to these empirical data. Thereby, 95%
249 confidence intervals are generated applying a bootstrap procedure with 1000 iterations to account for
250 extreme value statistical uncertainties. We find that the Teddy-Tool leads to an overestimation of
251 annual maximum precipitation. For the hourly duration, the differences are large with the confidence
252 intervals of the GEV hardly overlapping. For the longer durations, Teddy values approach the original
253 data, with noticeable differences only for the rare events with return periods above 5 years.



254

255 Figure 9: Extreme value statistical evaluation of sub-daily precipitation. The annual maxima of the
256 WFDE5 and Teddy are shown as dots. Additionally, GEV fits (lines) with 95% confidence intervals
257 (transparent areas and dashed lines) account for uncertainties. The Teddy-Tool is run with a DOY
258 window size of 11 days.



259

260 Figure 10: Pearson correlation coefficient for each year for sample location 29 and a DOY window size
 261 of 11 days. The scaling of the colorbar differs between variables.

262

263



264 **3. Discussion**

265 The Teddy-Tool allows for temporal disaggregation of daily climate model data. The disaggregation is
266 based on location and time specific empirical relationships between variables. The approach is well
267 suitable for all tested variables and results in high correlations (>0.9), except for precipitation (>0.5)
268 and wind speed (>0.75). Compared to other approaches, the advantage of the Teddy-Tool is that no
269 other input data is required rather than the daily climate model data. The Teddy-Tool is relatively
270 simple to apply, considers specific regional and seasonal features of the diurnal course of different
271 climate variables. Mass and energy are conserved and mean daily values of the climate model are
272 reproduced any time.

273 The spatial and temporal resolution of the results is determined by the provided temporal and spatial
274 resolution of the chosen reference data (WFDE5 used here). Longer available reanalysis time periods
275 extend the basic population for identifying the most similar weather conditions in the past and thus
276 could improve the results. Generally, also other reference data could be used, that provides higher
277 temporal or spatial resolution for a specific region.

278 The time window to find the most similar historical weather situations can be chosen in different sizes.
279 For most of the variables, we found small effects of time window adjustments, except for precipitation
280 and wind speed. The evaluation of different DOY window sizes reveals that a DOY window size of 11
281 can generally be recommended across all variables. Larger DOY windows should be avoided mainly in
282 arid regions, while shorter DOY windows generally lead to poorer representations of autocorrelation
283 and extreme events.

284 One limitation of the Teddy-Tool is the representation of extreme events, mainly for precipitation,
285 which is generally the most difficult variable for temporal disaggregation. We found that hourly
286 precipitation extremes are not always reproduced. For heavy daily precipitation events, Teddy
287 distributes the 24h-sums either correctly, too evenly or on too few hours. When distributing on too
288 few hours, extreme hourly intensities evolve, which may have never occurred or may even be
289 physically implausible. For temporal disaggregation of extreme precipitation, we recommend
290 dynamical downscaling via high-resolution climate models (Poschlod, 2021; Poschlod et al., 2021;
291 Zabel et al., 2012; Zabel and Mauser, 2013).

292 For the disaggregation of future climate projections using of the Teddy-Tool, we have the following
293 remarks: As the Teddy-Tool derives the relationships between sub-daily and daily values empirically
294 based on reanalysis data, future diurnal profiles, which are outside the historical range of diurnal
295 profiles, might possibly be not fully reproduced. However, this limitation is common for statistical
296 approaches, which are to be calibrated on historical data (Papalexiou et al., 2018). Nevertheless, due
297 to energy and mass conservation, climate trends in the daily climate signal are fully preserved. Hence,
298 applying Teddy for temporal disaggregation under climate change holds under the assumption that we
299 select the most similar day of the historical data and that this diurnal profile is representative for future
300 climatic conditions. However, this assumption might apply to a different degree for different variables.
301 We expect non-stationarity for the diurnal profiles due to changing weather patterns, shifts in rainfall
302 generating processes, and shifts in the seasonality, mainly for precipitation and wind. The daily course
303 of other variables, such as solar radiation and temperature might generally be less affected by a
304 warmer climate. Furthermore, global climate models at coarse resolutions generally do not represent
305 all processes to fully reproduce intraday variability. Teddy applies the diurnal profiles and intraday



306 variability from the WFDE5 data, which are bias-adjusted ERA5 reanalysis data that implicitly consider
307 finer scale effects than coarse-resolution global climate models (Cucchi et al., 2020). Thus, the
308 disaggregation process in Teddy is consistent with the bias adjustment in ISIMIP3.

309 Further possible developments include an improved inter-day connectivity. Despite the consideration
310 of precipitation classes, still abrupt changes over day changes are possible. A future introduction of
311 temperature classes and surface pressure classes in addition to the precipitation classes could help to
312 reduce this effect. Depending on the location of interest, also including climate modes or weather
313 patterns for the choice of the most similar day could improve the performance. Other optional future
314 developments could include the separation of direct and diffuse radiation, which is also a required
315 information for some impact models which is currently not provided by ISIMIP.

316 **Code availability**

317 The source code of the Teddy-Tool (v1.0) including preprocessed data, results of the cross-validation
318 and exemplary results for SSP 585 (2015 – 2100) and the UKESM1-0-L climate model for 30 samples
319 are provided via Zenodo (<https://doi.org/10.5281/zenodo.7679149>).

320 **Author contribution**

321 FZ: Conceptualization, Software, Methodology, Validation, Formal analysis, Resources, Data curation,
322 Writing - original draft, Visualization

323 BP: Methodology, Validation, Formal analysis, Writing - original draft, Visualization

324 **Competing interests**

325 The contact author has declared that none of the authors has any competing interests.

326 **Acknowledgements**

327 We acknowledge the methodological discussion with Stefan Lange from the Potsdam Institute of
328 Climate Impact Research (PIK).

329 **References**

- 330 Ailliot, P., Allard, D., Monbet, V., and Naveau, P.: Stochastic weather generators: an overview of
331 weather type models, *Journal de la société française de statistique*, 156, <https://doi.org/101-113>,
332 2015.
- 333 Beck, H. E., Zimmermann, N. E., McVicar, T. R., Vergopolan, N., Berg, A., and Wood, E. F.: Present and
334 future Köppen-Geiger climate classification maps at 1-km resolution, *Scientific Data*, 5, 180214,
335 <https://doi.org/10.1038/sdata.2018.214>, 2018.
- 336 Breinl, K. and Di Baldassarre, G.: Space-time disaggregation of precipitation and temperature across
337 different climates and spatial scales, *Journal of Hydrology: Regional Studies*, 21, 126-146,
338 <https://doi.org/10.1016/j.ejrh.2018.12.002>, 2019.
- 339 Buck, A. L.: New Equations for Computing Vapor Pressure and Enhancement Factor, *Journal of*
340 *Applied Meteorology and Climatology*, 20, 1527-1532, [https://doi.org/10.1175/1520-0450\(1981\)020<1527:Nefcvp>2.0.Co;2](https://doi.org/10.1175/1520-0450(1981)020<1527:Nefcvp>2.0.Co;2), 1981.
- 342 Byers, E., Gidden, M., Leclère, D., Balkovic, J., Burek, P., Ebi, K., Greve, P., Grey, D., Havlik, P., Hillers,
343 A., Johnson, N., Kahil, T., Krey, V., Langan, S., Nakicenovic, N., Novak, R., Obersteiner, M.,
344 Pachauri, S., Palazzo, A., Parkinson, S., Rao, N. D., Rogelj, J., Satoh, Y., Wada, Y., Willaarts, B., and
345 Riahi, K.: Global exposure and vulnerability to multi-sector development and climate change



- 346 hotspots, *Environmental Research Letters*, 13, 055012, <https://doi.org/10.1088/1748-9326/aabf45>, 2018.
- 347
- 348 Chen, D., Dai, A., and Hall, A.: The Convective-To-Total Precipitation Ratio and the “Drizzling” Bias in
349 *Climate Models*, *Journal of Geophysical Research: Atmospheres*, 126, e2020JD034198,
350 <https://doi.org/10.1029/2020JD034198>, 2021.
- 351 Colón-González, F. J., Sewe, M. O., Tompkins, A. M., Sjödin, H., Casallas, A., Rocklöv, J., Caminade, C.,
352 and Lowe, R.: Projecting the risk of mosquito-borne diseases in a warmer and more populated
353 world: a multi-model, multi-scenario intercomparison modelling study, *The Lancet Planetary*
354 *Health*, 5, e404-e414, [https://doi.org/10.1016/S2542-5196\(21\)00132-7](https://doi.org/10.1016/S2542-5196(21)00132-7), 2021.
- 355 Cucchi, M., Weedon, G. P., Amici, A., Bellouin, N., Lange, S., Müller Schmied, H., Hersbach, H., and
356 Buontempo, C.: WFDE5: bias-adjusted ERA5 reanalysis data for impact studies, *Earth Syst. Sci.*
357 *Data*, 12, 2097-2120, <https://doi.org/10.5194/essd-12-2097-2020>, 2020.
- 358 Debele, B., Srinivasan, R., and Yves Parlange, J.: Accuracy evaluation of weather data generation and
359 disaggregation methods at finer timescales, *Advances in Water Resources*, 30, 1286-1300,
360 <https://doi.org/10.1016/j.advwatres.2006.11.009>, 2007.
- 361 Degife, A. W., Zabel, F., and Mauser, W.: Climate change impacts on potential maize yields in
362 Gambella region, Ethiopia, *Regional Environmental Change*, <https://doi.org/10.1007/s10113-021-01773-3>, 2021.
- 363
- 364 Eyring, V., Bony, S., Meehl, G. A., Senior, C. A., Stevens, B., Stouffer, R. J., and Taylor, K. E.: Overview
365 of the Coupled Model Intercomparison Project Phase 6 (CMIP6) experimental design and
366 organization, *Geosci. Model Dev.*, 9, 1937-1958, <https://doi.org/10.5194/gmd-9-1937-2016>, 2016.
- 367 Förster, K., Hanzer, F., Winter, B., Marke, T., and Strasser, U.: An open-source MEteoroLogical
368 observation time series DISaggregation Tool (MELODIST v0.1.1), *Geosci. Model Dev.*, 9, 2315-
369 2333, <https://doi.org/10.5194/gmd-9-2315-2016>, 2016.
- 370 Franke, J. A., Müller, C., Minoli, S., Elliott, J., Folberth, C., Gardner, C., Hank, T., Izaurrealde, R. C.,
371 Jägermeyr, J., Jones, C. D., Liu, W., Olin, S., Pugh, T. A. M., Ruane, A. C., Stephens, H., Zabel, F., and
372 Moyer, E. J.: Agricultural breadbaskets shift poleward given adaptive farmer behavior under
373 climate change, *Global Change Biol.*, 28, 167-181, <https://doi.org/10.1111/gcb.15868>, 2022.
- 374 Golub, M., Thiery, W., Marcé, R., Pierson, D., Vanderkelen, I., Mercado-Bettin, D., Woolway, R. I.,
375 Grant, L., Jennings, E., Kraemer, B. M., Schewe, J., Zhao, F., Frieler, K., Mengel, M., Bogomolov, V.
376 Y., Bouffard, D., Côté, M., Couture, R. M., Debolskiy, A. V., Droppers, B., Gal, G., Guo, M., Janssen,
377 A. B. G., Kirillin, G., Ladwig, R., Magee, M., Moore, T., Perroud, M., Piccolroaz, S., Raaman Vinnaa,
378 L., Schmid, M., Shatwell, T., Stepanenko, V. M., Tan, Z., Woodward, B., Yao, H., Adrian, R., Allan,
379 M., Anneville, O., Arvola, L., Atkins, K., Boegman, L., Carey, C., Christianson, K., de Eyto, E.,
380 DeGasperi, C., Grechushnikova, M., Hejzlar, J., Joehnk, K., Jones, I. D., Laas, A., Mackay, E. B.,
381 Mammarella, I., Markensten, H., McBride, C., Özkundakci, D., Potes, M., Rinke, K., Robertson, D.,
382 Rusak, J. A., Salgado, R., van der Linden, L., Verburg, P., Wain, D., Ward, N. K., Wollrab, S., and
383 Zdorovennova, G.: A framework for ensemble modelling of climate change impacts on lakes
384 worldwide: the ISIMIP Lake Sector, *Geosci. Model Dev.*, 15, <https://doi.org/4597-4623>,
385 10.5194/gmd-15-4597-2022, 2022.
- 386 Görner, C., Franke, J., Kronenberg, R., Hellmuth, O., and Bernhofer, C.: Multivariate non-parametric
387 Euclidean distance model for hourly disaggregation of daily climate data, *Theoretical and Applied*
388 *Climatology*, 143, 241-265, <https://doi.org/10.1007/s00704-020-03426-7>, 2021.
- 389 Jägermeyr, J., Müller, C., Ruane, A. C., Elliott, J., Balkovic, J., Castillo, O., Faye, B., Foster, I., Folberth,
390 C., Franke, J. A., Fuchs, K., Guarin, J. R., Heinke, J., Hoogenboom, G., Iizumi, T., Jain, A. K., Kelly, D.,
391 Khabarov, N., Lange, S., Lin, T.-S., Liu, W., Mialyk, O., Minoli, S., Moyer, E. J., Okada, M., Phillips,
392 M., Porter, C., Rabin, S. S., Scheer, C., Schneider, J. M., Schyns, J. F., Skalsky, R., Smerald, A., Stella,
393 T., Stephens, H., Webber, H., Zabel, F., and Rosenzweig, C.: Climate impacts on global agriculture
394 emerge earlier in new generation of climate and crop models, *Nature Food*, 2, 873-885,
395 <https://doi.org/10.1038/s43016-021-00400-y>, 2021.
- 396 Kumar, D., Mishra, V., and Ganguly, A. R.: Evaluating wind extremes in CMIP5 climate models,
397 *Climate Dynamics*, 45, 441-453, <https://doi.org/10.1007/s00382-014-2306-2>, 2015.



- 398 Kunstmann, H. and Stadler, C.: High resolution distributed atmospheric-hydrological modelling for
399 Alpine catchments, *Journal of Hydrology*, 314, 105-124,
400 <https://doi.org/10.1016/j.jhydrol.2005.03.033>, 2005.
- 401 Lange, S.: Trend-preserving bias adjustment and statistical downscaling with ISIMIP3BASD (v1.0),
402 *Geosci. Model Dev.*, 12, 3055-3070, <https://doi.org/10.5194/gmd-12-3055-2019>, 2019.
- 403 Li, X., Meshgi, A., Wang, X., Zhang, J., Tay, S. H. X., Pijcke, G., Manocha, N., Ong, M., Nguyen, M. T.,
404 and Babovic, V.: Three resampling approaches based on method of fragments for daily-to-subdaily
405 precipitation disaggregation, *International Journal of Climatology*, 38, e1119-e1138,
406 <https://doi.org/10.1002/joc.5438>, 2018.
- 407 Liston, G. E. and Elder, K.: A Meteorological Distribution System for High-Resolution Terrestrial
408 Modeling (MicroMet), *Journal of Hydrometeorology*, 7, 217-234,
409 <https://doi.org/10.1175/jhm486.1>, 2006.
- 410 Liu, C., Ikeda, K., Thompson, G., Rasmussen, R., and Dudhia, J.: High-Resolution Simulations of
411 Wintertime Precipitation in the Colorado Headwaters Region: Sensitivity to Physics
412 Parameterizations, *Monthly Weather Review*, 139, 3533-3553, <https://doi.org/10.1175/MWR-D-11-00009.1>, 2011.
- 414 Mengel, M., Treu, S., Lange, S., and Frieler, K.: ATTRICI v1.1 – counterfactual climate for impact
415 attribution, *Geosci. Model Dev.*, 14, 5269-5284, <https://doi.org/10.5194/gmd-14-5269-2021>,
416 2021.
- 417 Mezghani, A. and Hingray, B.: A combined downscaling-disaggregation weather generator for
418 stochastic generation of multisite hourly weather variables over complex terrain: Development
419 and multi-scale validation for the Upper Rhone River basin, *Journal of Hydrology*, 377, 245-260,
420 <https://doi.org/10.1016/j.jhydrol.2009.08.033>, 2009.
- 421 Minoli, S., Jägermeyr, J., Asseng, S., Urfels, A., and Müller, C.: Global crop yields can be lifted by
422 timely adaptation of growing periods to climate change, *Nature Communications*, 13, 7079,
423 <https://doi.org/10.1038/s41467-022-34411-5>, 2022.
- 424 Orlov, A., Daloz, A. S., Sillmann, J., Thiery, W., Douzal, C., Lejeune, Q., and Schleussner, C.: Global
425 Economic Responses to Heat Stress Impacts on Worker Productivity in Crop Production,
426 *Economics of Disasters and Climate Change*, 5, 367-390, <https://doi.org/10.1007/s41885-021-00091-6>, 2021.
- 428 Orlov, A., et al.: Human heat stress could offset economic benefits of the CO2 fertilisation effect in
429 crop production. *Nature Communications: Under Review*, 2023.
- 430 Papalexioiu, S. M., Markonis, Y., Lombardo, F., AghaKouchak, A., and Foufoula-Georgiou, E.: Precise
431 Temporal Disaggregation Preserving Marginals and Correlations (DiPMaC) for Stationary and
432 Nonstationary Processes, *Water Resources Research*, 54, 7435-7458,
433 <https://doi.org/10.1029/2018WR022726>, 2018.
- 434 Park, H. and Chung, G.: A Nonparametric Stochastic Approach for Disaggregation of Daily to Hourly
435 Rainfall Using 3-Day Rainfall Patterns, *Water*, 12, 2306, 2020.
- 436 Portmann, F. T., Siebert, S., and Döll, P.: MIRCA2000—Global monthly irrigated and rainfed crop
437 areas around the year 2000: A new high-resolution data set for agricultural and hydrological
438 modeling, *Global Biogeochemical Cycles*, 24, <https://doi.org/10.1029/2008GB003435>, 2010.
- 439 Poschlod, B.: Using high-resolution regional climate models to estimate return levels of daily extreme
440 precipitation over Bavaria, *Nat. Hazards Earth Syst. Sci.*, 21, 3573-3598,
441 <https://doi.org/10.5194/nhess-21-3573-2021>, 2021.
- 442 Poschlod, B. and Ludwig, R.: Internal variability and temperature scaling of future sub-daily rainfall
443 return levels over Europe, *Environmental Research Letters*, 16, 064097,
444 <https://doi.org/10.1088/1748-9326/ac0849>, 2021.
- 445 Poschlod, B., Ludwig, R., and Sillmann, J.: Ten-year return levels of sub-daily extreme precipitation
446 over Europe, *Earth Syst. Sci. Data*, 13, 983-1003, <https://doi.org/10.5194/essd-13-983-2021>, 2021.
- 447 Poschlod, B., Hodnebrog, Ø., Wood, R. R., Alterskjær, K., Ludwig, R., Myhre, G., and Sillmann, J.:
448 Comparison and Evaluation of Statistical Rainfall Disaggregation and High-Resolution Dynamical



- 449 Downscaling over Complex Terrain, *Journal of Hydrometeorology*, 19, 1973-1982,
450 <https://doi.org/10.1175/jhm-d-18-0132.1>, 2018.
- 451 Reed, C., Anderson, W., Kruczkiwicz, A., Nakamura, J., Gallo, D., Seager, R., and McDermid, S. S.: The
452 impact of flooding on food security across Africa, *Proceedings of the National Academy of*
453 *Sciences*, 119, e2119399119, <https://doi.org/10.1073/pnas.2119399119>, 2022.
- 454 Sun, Y., Solomon, S., Dai, A., and Portmann, R. W.: How Often Does It Rain?, *Journal of Climate*, 19,
455 <https://doi.org/916-934>, 10.1175/jcli3672.1, 2006.
- 456 Tittensor, D. P., Novaglio, C., Harrison, C. S., Heneghan, R. F., Barrier, N., Bianchi, D., Bopp, L.,
457 Bryndum-Buchholz, A., Britten, G. L., Büchner, M., Cheung, W. W. L., Christensen, V., Coll, M.,
458 Dunne, J. P., Eddy, T. D., Everett, J. D., Fernandes-Salvador, J. A., Fulton, E. A., Galbraith, E. D.,
459 Gascuel, D., Guiet, J., John, J. G., Link, J. S., Lotze, H. K., Maury, O., Ortega-Cisneros, K., Palacios-
460 Abrantes, J., Petrik, C. M., du Pontavice, H., Rault, J., Richardson, A. J., Shannon, L., Shin, Y.-J.,
461 Steenbeek, J., Stock, C. A., and Blanchard, J. L.: Next-generation ensemble projections reveal
462 higher climate risks for marine ecosystems, *Nat Clim Change*, 11, 973-981,
463 <https://doi.org/10.1038/s41558-021-01173-9>, 2021.
- 464 Trinanés, J. and Martínez-Urtaza, J.: Future scenarios of risk of *Vibrio* infections in a warming planet:
465 a global mapping study, *The Lancet Planetary Health*, 5, e426-e435,
466 [https://doi.org/10.1016/S2542-5196\(21\)00169-8](https://doi.org/10.1016/S2542-5196(21)00169-8), 2021.
- 467 Verfaillie, D., Déqué, M., Morin, S., and Lafaysse, M.: The method ADAMONT v1.0 for statistical
468 adjustment of climate projections applicable to energy balance land surface models, *Geosci.*
469 *Model Dev.*, 10, 4257-4283, <https://doi.org/10.5194/gmd-10-4257-2017>, 2017.
- 470 Vormoor, K. and Skaugen, T.: Temporal Disaggregation of Daily Temperature and Precipitation Grid
471 Data for Norway, *Journal of Hydrometeorology*, 14, 989-999, [https://doi.org/10.1175/jhm-d-12-](https://doi.org/10.1175/jhm-d-12-0139.1)
472 [0139.1](https://doi.org/10.1175/jhm-d-12-0139.1), 2013.
- 473 Wang, K. and Clow, G. D.: The Diurnal Temperature Range in CMIP6 Models: Climatology, Variability,
474 and Evolution, *Journal of Climate*, 33, 8261-8279, <https://doi.org/10.1175/jcli-d-19-0897.1>, 2020.
- 475 Warszawski, L., Frieler, K., Huber, V., Piontek, F., Serdeczny, O., and Schewe, J.: The Inter-Sectoral
476 Impact Model Intercomparison Project (ISI-MIP): Project framework, *Proceedings of the National*
477 *Academy of Sciences*, 111, 3228-3232, <https://doi.org/10.1073/pnas.1312330110>, 2014.
- 478 Wehner, M., Lee, J., Risser, M., Ullrich, P., Gleckler, P., and Collins, W. D.: Evaluation of extreme sub-
479 daily precipitation in high-resolution global climate model simulations, *Philosophical Transactions*
480 *of the Royal Society A: Mathematical, Physical and Engineering Sciences*, 379, 20190545,
481 <https://doi.org/10.1098/rsta.2019.0545>, 2021.
- 482 Zabel, F. and Mauser, W.: 2-way coupling the hydrological land surface model PROMET with the
483 regional climate model MM5, *Hydrology and Earth System Sciences*, 17, 1705-1714,
484 <https://doi.org/10.5194/hess-17-1705-2013>, 2013.
- 485 Zabel, F., Mauser, W., Marke, T., Pfeiffer, A., Zängl, G., and Wastl, C.: Inter-comparison of two land-
486 surface models applied at different scales and their feedbacks while coupled with a regional
487 climate model, *Hydrology and Earth System Sciences*, 16, 1017-1031,
488 <https://doi.org/10.5194/hess-16-1017-2012>, 2012.
- 489 Zabel, F., Müller, C., Elliott, J., Minoli, S., Jägermeyr, J., Schneider, J. M., Franke, J. A., Moyer, E., Dury,
490 M., Francois, L., Folberth, C., Liu, W., Pugh, T. A. M., Olin, S., Rabin, S. S., Mauser, W., Hank, T.,
491 Ruane, A. C., and Asseng, S.: Large potential for crop production adaptation depends on available
492 future varieties, *Global Change Biol*, 27, 3870-3882 <https://doi.org/10.1111/gcb.15649>, 2021.
- 493 Zhao, W., Kinouchi, T., and Nguyen, H. Q.: A framework for projecting future intensity-duration-
494 frequency (IDF) curves based on CORDEX Southeast Asia multi-model simulations: An application
495 for two cities in Southern Vietnam, *Journal of Hydrology*, 598, 126461,
496 <https://doi.org/10.1016/j.jhydrol.2021.126461>, 2021.